

Assessing nanoparticle-enabled dsRNA delivery for oral RNAi in two orthopteran pests: *Schistocerca gregaria* and *Melanoplus sanguinipes*[☆]

Seema Rana^{a,*}, Changsun Kang^b, Seonghyun Ryu^b, Derek A. Woller^c, Dongin Kim^b, Hojun Song^{a,*}

^a Department of Entomology, Texas A&M University, College Station, TX, USA

^b Department of Pharmaceutical Sciences, The University of Oklahoma Health Sciences, Center, Oklahoma City, OK, USA

^c USDA-APHIS-PPQ-PEIP-Imports, Regulations, and Manuals, Lexington, KY, USA

ARTICLE INFO

Keywords:

Locust
RNAi efficiency
Oral feeding
Poly lactic-co-glycolic acid
Poly(L-arginine)-polyethylene glycol

ABSTRACT

Locusts and pest grasshoppers (Orthoptera: Acrididae) cause significant economic losses to agricultural crops and rangeland forage and can even cause humanitarian crises during periodic plagues. Current management methods for these insects rely heavily on broad-spectrum chemical insecticides and growth regulators, which can affect non-target organisms and may eventually develop resistance in the targeted species. Therefore, we assessed the potential of RNA interference (RNAi)-based alternative strategies that could supplement the current management methods. In insects, RNAi efficiency is known to vary with the method of double-stranded RNA (dsRNA) delivery. In this study, we tested two different delivery methods (injection and oral feeding) in the desert locust (*Schistocerca gregaria*) and the migratory grasshopper (*Melanoplus sanguinipes*) and showed that both species are sensitive to the injection but not to the oral feeding of dsRNA, likely due to high nuclease activity or poor uptake in the midgut. To address these limitations, we explored the utility of using nanoparticles that are often used for drug delivery in humans as a carrier (poly lactic-co-glycolic acid [PLGA] and poly(L-arginine)-polyethylene glycol [PLA-PEG]) for orally delivering dsRNA to the insect pests. Although the PLGA nanoparticles successfully permeated the digestive system into the hemolymph and the PLA-PEG-dsRNA complexes remained stable in the midgut juice and were detected in the fat body, neither dsRNA-encapsulating nanoparticle elicited gene knockdown upon oral feeding. These results suggest that nanoparticle-based oral delivery improves dsRNA stability and midgut permeation. However, additional barriers must be overcome to achieve efficient oral RNAi in these orthopteran pest species.

1. Introduction

Orthopteran pests (locusts and grasshoppers) cause significant economic damage around the world, and the currently used control methods heavily rely on chemical pesticides. The desert locust (*Schistocerca gregaria* (Forskål)) is one of the most notorious migratory pests known to humanity, forming enormous swarms that devastate crops and cause famines in parts of Africa and the Middle East (Food and Agriculture Organization (FAO), 2020). Locust outbreaks pose a significant threat to global food security (Le Gall et al., 2019), second only to drought in terms of reducing crop productivity (Alessandro et al., 2015). The 2019–2020 upsurge of the desert locust affected 30 countries in East Africa and the Middle East, which was considered the worst in the last

70 years (FAO, 2020), with over a million hectares treated with organophosphates and pyrethroids to control these outbreaks (Newsom et al., 2021). A new outbreak in 2025 is currently spreading from Niger and Sudan into Northwestern Africa (FAO, 2025), further underscoring the ongoing threat posed by this pest. In North America, the migratory grasshopper (*Melanoplus sanguinipes* (Fabricius)) is a key pest in the western United States, causing more forage loss than any other grasshopper species (Pfadt, 2002; United States Department of Agriculture Animal and Plant Health Inspection Service (USDA APHIS), 2019). Its mixed diet habit, feeding on both grasses and forbs, allows it to consume a wide variety of crops, including cereals, vegetables, and rangeland plants (Pfadt, 2002; Murray, 2016). *M. sanguinipes* outbreak populations can reach 80 individuals per square yard (Murray, 2016). The economic

[☆] This article is part of a special issue entitled: 'Methods for RNAi-mediated pest control' published in Journal of Insect Physiology.

* Corresponding authors.

E-mail addresses: seema.rana@ag.tamu.edu (S. Rana), Hojun.Song@ag.tamu.edu (H. Song).

value of rangelands for livestock forage, recreation, carbon sequestration, and other ecosystem services is estimated to range from \$10.7 billion to \$21.2 billion, based on a 2012 economic analysis prepared by the University of Wyoming through a cooperative agreement with APHIS (USDA APHIS, 2024). Current management methods for grasshoppers on rangeland habitats in the U.S. include aerial application of chemical insecticides, including liquid diflufenzuron and carbaryl baits (USDA APHIS, 2024). However, in general, the widespread use of chemical insecticides raises concerns about human health, non-target effects, loss of biodiversity, and, potentially, the development of resistance (USDA APHIS, 2019; Sparks et al., 2021). Alternatively, Mycoinsecticides (entomopathogenic fungi) have been shown to be effective, but they are slow in action, have high production costs, and can affect non-target orthopteran insects (USDA APHIS, 2019). Therefore, there is an urgent need to develop an effective and environmentally sustainable alternative management method. This study addresses this need by exploring RNA interference (RNAi) as a potential tool for the management of these two economically important orthopteran pests.

RNAi offers a promising insect management strategy because of its capacity to knock down the expression of essential genes in insects to induce low fitness or mortality and because of its target-specific nature (Joga et al., 2016). However, the application of RNAi as a management tool has some practical limitations, especially in terms of the delivery of double-stranded RNA (dsRNA) into the pests (Price and Gatehouse, 2008; Cooper et al., 2019; Zhu and Palli, 2020). While oral delivery of dsRNA is the most straightforward way of introducing dsRNA, it is not known to be effective in causing RNAi response in many insects, including locusts and grasshoppers. This inefficiency is largely due to the presence of double-stranded ribonucleases (dsRNases) in their midgut that can rapidly degrade ingested dsRNA, thereby reducing RNAi efficiency (Luo et al., 2013; Wynant et al., 2014; Singh et al., 2017; Song et al., 2017; Spit et al., 2017; Song et al., 2019). Previous studies have shown that orally ingested dsRNA can be protected by encapsulating it within nanoparticles, which help prevent degradation, thereby enhancing cellular uptake and ultimately improving RNAi efficiency (Joga et al., 2016; Pugsley et al., 2021). Several nanoparticles have been explored, including chitosan (Zhang et al., 2010, 2015), cationic core-shell fluorescent nanoparticles (He et al., 2013), guanilate polymers (Christiaens et al., 2018), carbon nanotubes (Edwards et al., 2020), block copolymer, and cell-penetrating peptides like poly(ethylene glycol)-polylysine (Laisney et al., 2020; Lu et al., 2022; Vogel et al., 2023). These systems have demonstrated potential for improving dsRNA delivery by oral feeding in various insect species.

Poly(lactic-co-glycolic acid) (PLGA) is an FDA-approved polymer that has shown promise for drug and gene delivery due to its biocompatibility and ability to protect nucleic acids from degradation (Wise et al., 1976; Gilding and Reed, 1979; Makadia and Siegel, 2011). PLGA forms emulsion-based nanoparticles that are biodegradable and offer controlled release of the encapsulated material (Hausbergert and Deluca, 1995; Makadia and Siegel, 2011). In recent decades, polyamino acids have gained significant attention due to their non-toxic nature, biocompatibility, nutritional benefits, and pharmacological effectiveness (Wu et al., 2008). Among these, cationic polyamino acids are particularly promising, as their positive charge facilitates interaction with genetic material through electrostatic forces. This charge also enables them to adhere to cell surfaces, thereby enhancing cellular uptake. Poly(L-arginine), one of the cationic polyamino acids, is known for its efficient cellular entry (Mitchell et al., 2000; Wu et al., 2008) and has been used for siRNA delivery in various systems (Zhang et al., 2006; Noh et al., 2010). Interestingly, in insects, poly(L-arginine) nanoparticles have also shown promise in improving RNAi efficiency in fall armyworm (*Spodoptera frugiperda* (Smith)), although these studies were limited to cell lines (Laisney et al., 2020).

In the pharmaceutical industry, enhancing drug delivery often involves attaching a safe and hydrophilic polymer, such as polyethylene glycol (PEG). Similarly, researchers have combined PEG with another

polyamino acid, such as polylysine, to improve RNAi efficiency in the migratory locust (*Locusta migratoria* (Linnaeus)) (Lu et al., 2022). However, poly(L-arginine) is alternatively known to be better at penetrating cells, relatively cost-effective to produce at a large scale, and biodegradable, making it more suitable for agricultural applications compared to polylysine (Mitchell et al., 2000; Robison et al., 2016). Based on these advantages, we have chosen to create complexes by combining poly(L-arginine) with PEG nanoparticles.

In this study, we used PLGA and poly(L-arginine)-polyethylene glycol (PLA-PEG) to form novel nanoparticles for oral dsRNA delivery in *S. gregaria* and *M. sanguinipes*. We evaluated these nanoparticle formulations for their stability, permeability, and release kinetics in hemolymph and midgut juice. To assess their potential to improve RNAi, we tested the hypothesis that PLGA-dsRNA and PLA-PEG-dsRNA could improve oral RNAi efficiency in both species. In addition, we explored an RNAi-of-RNAi approach by knocking down double-stranded ribonucleases 2 (*dsRNase2*) to improve dsRNA stability and uptake in the digestive system. Both injection and oral feeding methods were used to evaluate RNAi efficiency in these orthopteran pests.

2. Materials and methods

2.1. Transcriptome sequencing and assembly of *Melanoplus sanguinipes*

As genomic resources for *M. sanguinipes* were not available at all, we first generated a *de novo* transcriptome to identify target genes in *M. sanguinipes* for our experiments. In October 2021, we received live specimens of *M. sanguinipes* collected from the San Carlos Apache Indian Reservation in Arizona by two teams within the United States Department of Agriculture (USDA)'s Animal and Plant Health Inspection Service (APHIS)-Plant Protection and Quarantine (PPQ) (Phoenix, AZ, USA). Some of these specimens were snap-frozen in liquid nitrogen and stored in a -80°C freezer for transcriptome sequencing. To generate tissue-specific transcriptomes, three adult females were dissected, and RNA was extracted from the head, thorax, and abdomen tissues. Total RNA was extracted using a Trizol method (Chomczynski and Mackey, 1995), followed by column purification with DNase treatment using the RNeasy mini kit (Qiagen, Hilden, Germany) to remove any residual genomic DNA. The concentration and purity of extracted RNA were measured using a spectrophotometer (DeNovix DS-11). RNA samples were then sent to Novogene (Sacramento, CA, USA) for library preparation and sequencing.

A total of nine sequencing libraries were prepared using the NEB-Next® Ultra™ RNA Library Prep Kit for Illumina® (New England Biolabs, Ipswich, MA, USA) according to the manufacturer's instructions. Index codes were added to each sample to allow for sequence attribution. Library fragments of approximately 150–200 bp were selected using the AMPure XP system (Beckman Coulter, Beverly, CA, USA). The quality of each library was assessed using the Agilent Bioanalyzer 2100 system. Sequencing was carried out on an Illumina NovaSeq 6000 platform, generating 150 bp paired-end reads at Novogene.

Raw reads were initially processed for quality control using fastp (Version 0.20.1) to remove low-quality sequences and filter the high-quality reads. Clean reads from all biological replicates and tissue samples were pooled for a *de novo* transcriptome assembly, performed using Trinity (Version 2.9.1) with the parameter `min_kmer_cov` set to 2, while all other parameters were left at default settings. To further refine the assembly, CD-HIT-EST (Version 4.8.1) was used to cluster similar contigs, with word size set to 8 and the similarity threshold set to 0.95. Assembly quality was evaluated using Transrate (Version 1.0.3) to assess contig metrics, while the composition quality of the assembled transcriptome was analyzed using BUSCO (Benchmarking Universal Single-Copy Orthologs, Version 4.1.2).

2.2. Insect rearing regime

Both *S. gregaria* and *M. sanguinipes* were bred and maintained under crowded conditions at 30 °C with a 12 h light/12 h dark cycle at the USDA-approved containment facility in the Department of Entomology at Texas A&M University (College Station, TX, USA). The colonies of both species were established from the egg pods provided by Arizona State University under a USDA-APHIS-PPQ permit (P526P-22-06735). *Schistocerca gregaria* were housed in plastic cages (55 X 35 X 30 cm) with mesh panels on the top and bottom for ventilation, and a cotton sleeve opening at the front for easy access. In contrast, *M. sanguinipes* were housed in smaller cages (24.5 X 24.5 X 24.5 cm) with polyester mesh panels on all sides and a front opening sleeve for accessibility. The insects were fed with fresh wheatgrass and wheat bran daily. For *S. gregaria* experiments, freshly molted last instar nymphs were separated from the common cages and individually kept in 16 oz. plastic deli cups. Similarly, freshly molted last instar nymphs were used for all *M. sanguinipes* experiments. The nymphs were starved for 24 hrs before the experiments.

2.3. RNA extraction and dsRNA synthesis

Total RNA was extracted from a single nymphal head or thorax tissues using the Trizol method as described above. The extracted RNA was then reverse transcribed into cDNA using an iScript cDNA synthesis kit (Biorad, Hercules, CA, USA). PCR amplification was performed using the *M. sanguinipes* gene-specific primers (Table 1) and primers for *S. gregaria* from Wynant et al. (2012; 2014). The thermal cycling conditions consisted of an initial denaturation step at 94 °C for 2 min, followed by 10 cycles of 94 °C for 30 s, 55–60 °C for 30 s, and 72 °C for 1:30 min. This was followed by 25 cycles of 94 °C for 30 s, 69 °C for 30 s, and 72 °C for 1:30 min, with a final extension at 72 °C for 2 min. The resulting PCR products were purified using Monarch PCR and DNA Clean Up Kit (New England Biolabs, Ipswich, MA, USA) according to the manufacturer's protocol. These purified PCR products were then used as templates for dsRNA synthesis of the target genes, utilizing the MEGAscript RNAi Kit

Table 1
Primer sequences used in this study.

Gene name (accession number)	Sequence (5'-3')	Amplicon Size (bp)
dsGAPDH (PQ638923)	F: taatacgactcactatagggCGACCCATGGCAAGTTCAAG R: taatacgactcactatagggGTAGCAGTGACAGCATGCAC	400
dsCHS1 (PQ638924)	F: taatacgactcactatagggGGTGCCTGAAGTGGGTTTCAT R: taatacgactcactatagggATAGTTCTCCACCCAGCCAC	400
dsSec23 (PQ638925)	F: taatacgactcactatagggCCGAGCAGCAATAAATGGGC R: taatacgactcactatagggTTCCACTGACAAGTACCGCC	333
dsAChE (PQ638922)	F: taatacgactcactatagggCTTCGAGTACACCGACTGGG R: taatacgactcactatagggTAGTTGATCTCGTCGCCGTG	222
GAPDH	F: GAAGCTGCTGAGGTCCTTT R: GAGTGGGATGCTGCCTTAG	120
CHS1	F: TCACAGTTGCGGAAGGACAA R: AACCCACTTCAGGCACCAAA	145
Sec23	F: AAGCAGCGGCAGTTTTGATG R: GAGCATCCGGTCTATCCAGC	92
AChE	F: GGCGACGAGATCAACTACGT R: TTCCCGTCTTGGCGAAGTT	122
RpL5 (PQ638926)	F: TTCGTGCCAATCCAGATCGA R: CCTTCTTCTGGGCGATCCTG	120
RpL32 (PQ638927)	F: ACCATCCCCGATTTCCGTTT R: ATACACCGGACGAATCGCC	120

(Thermo Fisher Scientific, Waltham, MA, USA) according to the standard protocol. For non-target control in all experiments, dsRNA of *GFP* was synthesized using a TOPO GFP plasmid (Addgene, Watertown, MA, USA).

2.4. Testing RNAi efficiency

We selected the following four genes for developing dsRNAs: Glyceroldehyde 3 phosphate dehydrogenase (*GAPDH*), Chitin synthase 1 (*CHS1*), Secretory 23 (*Sec23*), and Acetylcholinesterase (*AChE*). Orthologs for the target genes from *S. gregaria* and *L. migratoria* were identified in the *M. sanguinipes* transcriptome using a BLAST search in Geneious Version 2022.2.2 (Dotmatics, Boston, MA, USA). The BLAST hits with high query coverage and pairwise identity were selected and verified through a secondary BLAST search against the NCBI database. The identified sequences of these target genes were used for dsRNA synthesis in subsequent RNAi experiments. The systemic RNAi response via injection in *S. gregaria* is well-known and the effective dsRNA dose for inducing RNAi is well-characterized (Wynant et al. 2012), but RNAi had never been applied to *M. sanguinipes*. Thus, we first performed a dose-dependent response study for *M. sanguinipes* by diluting dsRNA of *GAPDH/GFP* in locust saline solution to the final doses of 50, 100, 500, and 1000 ng. A volume of 5 µl of different doses of dsGAPDH and dsGFP was injected into the abdominal segment of the last nymphal instar, with 10 nymphs per dose per gene, to characterize the dose-dependent RNAi response.

2.5. Injection and oral feeding of naked dsRNA

We tested two different methods of dsRNA delivery— injection and oral feeding—using the RNAi-of-RNAi approach. This approach involved knocking down *dsRNase2* first, followed by *GAPDH*, with each method tested independently. To determine the optimal time point for the RNAi-of-RNAi experiments, we injected 10 µg of *dsdsRNase2* or *dsGFP* into 48 *S. gregaria* nymphs (6 nymphs per time point per gene). Midgut tissues were dissected at 24, 48, 72, and 96 h after injection, and the mRNA levels of *dsRNase2* were quantified via RT-qPCR.

For the *S. gregaria* experiment, a total of 18 nymphs were used, divided into three groups: GFP_GFP (negative control), GFP_GAPDH (single treatment), and *dsRNase2_GAPDH* (combination treatment). This three-group design was used for the subsequent RNAi-of-RNAi experiments. The *dsRNase2_GAPDH* group received an initial injection of 10 µg of *dsdsRNase2*, while the GFP_GFP and GFP_GAPDH received 10 µg of *dsGFP*. After 24 h of initial injection, 25 µg of *dsGAPDH* was injected into the GFP_GAPDH and *dsRNase2_GAPDH* groups, while 25 µg of *dsGFP* was injected into the GFP_GFP group. Injections were done with a 20 µl volume of dsRNA into the 2nd abdominal segment using a Hamilton microsyringe (700 series, 705RN, 50 µl, Sigma Aldrich, St. Louis, MO, USA) with a 22-gauge needle. Similarly, for oral feeding, *dsGFP/dsdsRNase2* was fed first, followed by *dsGFP/dsGAPDH* in a consecutive manner. The same doses of dsRNAs in 20 µl were applied onto lettuce discs (3 cm diameter), which were then air-dried for 5–10 min before being fed to the nymphs. After 72 h from the second injection or oral feeding, tissues (head, thorax, and midgut) were dissected, snap-frozen in liquid nitrogen, and stored at –80 °C for subsequent RT-qPCR analysis. In all the following experiments, the tissues were processed in the same way for RT-qPCR analysis.

For *M. sanguinipes*, the effect of oral feeding of naked dsRNA was studied by feeding 1 µg of dsRNA targeting specific genes (*GAPDH*, *CHS1*, and *GFP*) to the nymphal instar, with 6 nymphs per gene. After 72 h, the head and thorax were dissected for further RT-qPCR analysis.

2.6. Injection followed by oral feeding of naked dsRNA

We also performed the RNAi-of-RNAi approach by combining dsRNA delivery methods— injection followed by oral feeding using 18

S. gregaria (6 nymphs per group). The dsRNase2_GAPDH group received 10 µg of dsRNase2 by injection, while the GFP_GFP and GFP_GAPDH groups were injected with 10 µg of dsGFP. After 24 h, 25 µg of dsGAPDH was fed to the GFP_GAPDH and dsRNase2_GAPDH groups, and 25 µg of dsGFP was fed to the GFP_GFP group. Tissues (head, thorax, and midgut) were collected 72 h after feeding for further RT-qPCR analysis.

2.7. Preparation of PLGA-dsRNA and PLA-PEG-dsRNA

We followed the protocol for synthesizing PLGA-dsRNA detailed in Rana et al. (2023). Briefly, dsRNA (100 µg) was emulsified in 1 ml dichloromethane (DCM) (Sigma Aldrich, St. Louis, MO, USA) containing 100 mg PLGA using a probe ultrasonicator for 10 s on an ice bath. Primary emulsion was added to 2 ml 5 % polyvinyl alcohol (PVA) solution (Sigma Aldrich, St. Louis, MO, USA), then sonicated for 10 s on an ice bath. The emulsion was transferred to the 0.25 % PVA solution (100 ml) and stirred for 3 h to remove DCM. The dsRNA-encapsulated PLGA nanoparticles were washed in MilliQ water 3 times and resuspended, and their particle size and distribution were assessed using dynamic light scattering (DLS) with a particle size analyzer (ZetaPALS, Brookhaven Instruments, Holtsville, NY, USA). To synthesize PLA-PEG-dsRNA, mPEG-NHS (2 mg) (Sigma Aldrich, St. Louis, MO, USA) and poly(L-arginine) (5 mg) (Sigma Aldrich, St. Louis, MO, USA) were dissolved in 2 ml of DI water. The solution was stirred overnight, and byproducts were removed by the membrane dialysis method. A lyophilization process was conducted to obtain PLA-PEG. PLA-PEG and dsRNA were mixed in a 10:1 (W/W) ratio and resuspended in DI water to formulate dsRNA-loaded nanoparticles. The resulting nanoparticles were characterized using a Nanoparticle tracking analysis (NTA) (NS300, Malvern Instruments Ltd., Malvern, UK). The scheme for formulating PLA-PEG-dsRNA is depicted in Fig. 2A.

The morphology of naked dsRNA and PLA-PEG-dsRNA was analyzed using a Transmission Electron Microscope (TEM). Hydrophilized copper grids were prepared via glow discharge, and samples were stained with 2 % uranyl acetate. Grids were incubated with stained samples for 1 min, blotted onto filter paper, and air-dried for 30 min. TEM imaging was conducted using an FEI TEM at Texas A&M University, Veterinary Medicine & Biomedical Sciences (College Station, TX, USA).

2.8. Release kinetics of coumarin in hemolymph from PLGA-coumarin

To develop efficient PLGA-dsRNA nanoparticles, we first tested the permeability and release kinetics of different molecular weights of PLGA nanoparticles, which could protect and release the encapsulated dsRNA consistently upon crossing the midgut. We used coumarin dye as a proxy for dsRNA and encapsulated it within PLGA nanoparticles of three different molecular weights: low (7–20 kDa) (11088–7–20 k, Nanosoft Biotechnology LLC, NC, USA), medium (50–70 kDa) (11088–50–70 k, Nanosoft Biotechnology LLC, NC, USA), and high (70–100 kDa) (11088 70–100 k, Nanosoft Biotechnology LLC, NC, USA). This method was adapted from Rana et al. (2023). After producing the nanoparticles, 50 µl of the PLGA-coumarin was applied onto lettuce discs and allowed to dry. The treated discs were then fed to ten 24 h-starved nymphs of both species. Hemolymph was collected from each nymph at various time points: 12, 24, 48, 72, 96, 120, and 144 h after feeding in *S. gregaria*, and 3 and 6 h after feeding in *M. sanguinipes*. To quantify the coumarin dye in the hemolymph, a multimode plate reader (Molecular Devices Co., San Jose, CA, USA) was used, with an excitation wavelength at 440 nm and an emission wavelength at 534 nm.

2.9. Stability of PLA-PEG-dsRNA in *S. gregaria* midgut juice

We tested the stability of the PLA-PEG-dsRNA in the midgut juice. The abdomen of *S. gregaria* was dissected, and midgut tissues were isolated from five nymphs. The isolated midguts were then centrifuged at 16,000 g for 20 min at 4 °C. The supernatant was collected and used for

further analysis. The midgut juice was diluted 1:32 with saline, and dsGAPDH (1 µg) was incubated for 0 and 0.5 h, while PLA-PEG-dsGAPDH (1 µg) was incubated for 0, 0.5, 1, 2, and 3 h at room temperature. Samples were then analyzed on a 1 % agarose gel to assess dsRNA degradation over time.

2.10. Injection followed by oral feeding of PLGA-dsRNA

To test whether PLGA encapsulation could improve the RNAi response after oral delivery, we first performed the RNAi-of-RNAi approach by injection followed by oral feeding of PLGA-dsRNA in both species. A total of 18 nymphs (6 nymphs per group) were used. We injected 10 µg of dsRNase2 into the dsRNase2_GAPDH group and 10 µg of dsGFP into the control group. After 48 h, 25 µg of PLGA-dsGAPDH was fed to the GFP_GAPDH and dsRNase2_GAPDH groups, while 25 µg of PLGA-dsGFP was fed to the GFP_GFP group. A second dose of PLGA-dsGAPDH or PLGA-dsGFP was fed 24 h later. Tissues (head, thorax, and midgut) were dissected 96 h after the second feeding for further analysis.

2.11. Oral feeding of PLA-PEG-dsRNA

Because the encapsulation of dsRNA by polyamino acid conjugated with PEG alone was shown to protect dsRNA from degradation and improve cellular uptake (Lu et al., 2022), we tested PLA-PEG encapsulated dsGAPDH nanoparticles by oral feeding in *S. gregaria* (10 nymphs per gene) in inducing RNAi response. Initially, 10 µg PLA-PEG-dsGAPDH was fed to the treatment group, while 10 µg of PLA-PEG-dsGFP was fed to the control group. After 24 and 48 h, additional doses of 10 µg were fed as a boost. Tissues (head and thorax) were dissected at 72 h after the first feeding for further analysis. To test different time points and determine whether long-term feeding would result in a knockdown, a separate experiment was conducted where 5 µg of PLA-PEG-dsGAPDH or dsGFP was fed for 6 consecutive days, and tissues were dissected at 24 and 72 h after the last feeding for further analysis.

In *M. sanguinipes*, we developed PLA-PEG nanoparticles of GAPDH, CHS1, Sec23, and AChE. These nanoparticles were then fed orally to 50 starved *M. sanguinipes* nymphs, with 10 nymphs per gene. Initially, we fed 10 µg of the PLA-PEG-dsRNA encapsulating targeted genes on the first day. The same dose was fed additionally after 24 and 48 h. As a control, we fed the PLA-PEG-dsGFP. After 72 h from the first feeding, we dissected the tissues for further analysis. The same experimental approach used in *S. gregaria* for testing different time points and long-term feeding was repeated in *M. sanguinipes*. In this experiment, we fed 5 µg of the PLA-PEG-dsRNA of GAPDH and Sec23 for 5 consecutive days and dissected the tissues at 24 and 48 h after the last feeding for further analysis.

2.12. RT-qPCR analysis

Total RNA was extracted from three to five nymphal head, thorax, or midgut tissues using the same protocol mentioned above. Each individual tissue is considered a biological replicate. cDNA was synthesized using an iScript cDNA synthesis kit (Biorad, Hercules, CA) and used as a template to perform qPCR amplification on CFX Connect Real-Time PCR Systems (Bio-rad, Hercules, CA) using gene-specific primers (Table 1). Each qPCR reaction was performed with two technical replicates and three to five biological replicates and contained 10 µl of SYBR Green supermix (Bio-rad, Hercules, CA), 500 nM primers, and nuclease-free water to make up the total volume of 20 µl. The thermal cycling included initial denaturation for 3 min at 95 °C, followed by 40 cycles at 95 °C for 10 s and 60 °C for 30 s. No-template control and no-reverse transcriptase control were included to check for reaction mixture and DNA contamination, respectively. The relative mRNA level was analyzed using the CFX Manager 2.1 (Bio-rad, Hercules, CA) and further with the $2^{-\Delta\Delta CT}$ method (Livak and Schmittgen, 2001). The results were normalized using two reference genes, *EF1a* and *Ubc10* for *S. gregaria*;

RpL5 and *RpL32* for *M. sanguinipes*. All data were statistically analyzed using Student's *t*-test or one-way ANOVA, followed by Tukey's test ($p < 0.05$) (in R, Version 4.2.1).

2.13. Uptake of Cy3 labeled PLA-PEG-dsRNA into fat body cells

To assess the uptake of PLA-PEG-dsRNA nanoparticles from the insect digestive system, PLA-PEG was synthesized and fluorescently-labeled by attaching cyanine 3 (Cy3) with a poly-L-arginine backbone, and we conducted experiments with *S. gregaria* and *M. sanguinipes*. We labeled PLA instead of dsRNA to ensure that this assay was not compromised by the potential dsRNA degradation. Nymphs were orally fed with these labeled nanoparticles while the control nymphs were not fed. After 24 h, we dissected and fixed their fat body tissues using 4 % para-formaldehyde (Thermo Fisher Scientific, Waltham, MA, USA). Subsequently, the fixed tissues were permeabilized with 0.3 % Triton X-100 (Sigma Aldrich, St. Louis, MO, USA) at room temperature for 30 min. F-actin staining was carried out for 30 min of incubation with Alexa Fluor 488 phalloidin (Thermo Fisher Scientific, Waltham, MA, USA), followed by nucleus staining using Hoechst 33342 (Thermo Fisher Scientific, Waltham, MA, USA) for 10 min. Prepared tissues were mounted on glass slides and imaged using an Olympus Fluoview laser scanning confocal microscope at the Integrated Microscopy and Imaging Laboratory, Texas A&M College of Medicine (College Station, TX, USA).

3. Results

3.1. *Melanoplus sanguinipes* transcriptome assembly

About 98 % of the total reads from all the samples passed the quality filters (phred quality \geq Q30), as detailed in [Supplementary Table 1](#). The high-quality reads were pooled and assembled into a *de novo* transcriptome assembly using Trinity. The transcriptome assembly comprised 309,635 contigs, with a quality metric N50 value of 747 and contigs ranging between 200 and 13,214 bp ([Supplementary Table 2](#)). The assessment of assembly completeness using BUSCO against the *insecta_odb10* lineage (creation date: 2019-11-20) revealed a completeness score of 92.4 %, indicating robust coverage of expected gene content ([Supplementary Table 3](#)). This Transcriptome Shotgun Assembly (TSA) project has been deposited at DDBJ/EMBL/GenBank under the accession GKDM00000000. The version described in this paper is the first version, GKDM1000000.

3.2. Sensitivity to injection vs. refractoriness to oral feeding of naked dsRNA

In both species, *S. gregaria* and *M. sanguinipes*, the response to dsRNA delivery varied between injections and oral feeding methods. Injections of naked dsRNA resulted in a significant knockdown of *GAPDH* in both head and thorax tissues, with 20 to 25-fold reduction observed in the GFP_GAPDH and dsRNase2_GAPDH groups ([Fig. 1A](#)). Similarly,

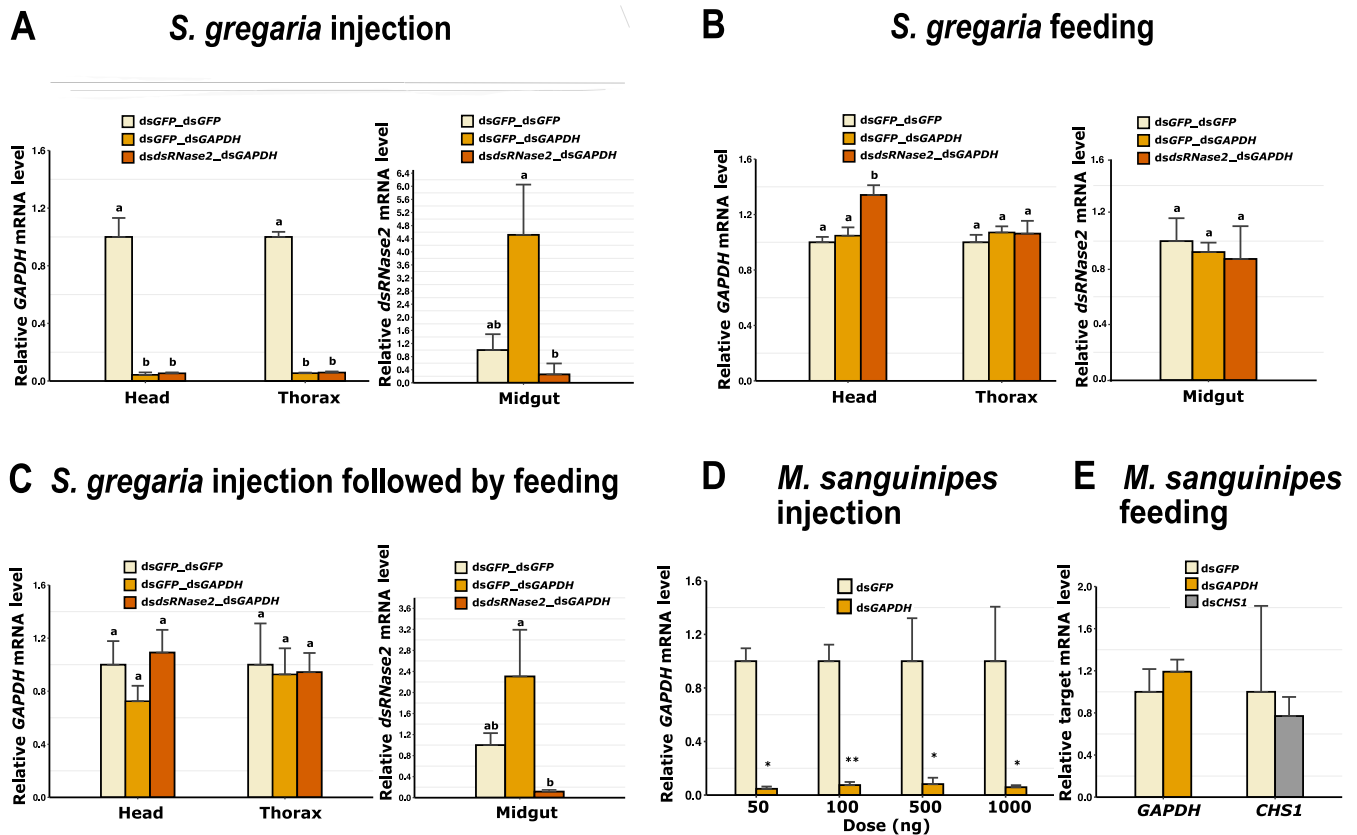


Fig. 1. Effect of injection and oral feeding of naked dsRNA in *S. gregaria* and *M. sanguinipes*. A. Effect of injection of dsRNA in *S. gregaria* in head, thorax and midgut tissues. B. Effect of oral feeding of naked dsRNA in *S. gregaria* in head, thorax and midgut tissues. C. Effect of injection of dsdsRNase2 followed by oral feeding of dsGAPDH in *S. gregaria* in head, thorax and midgut tissues. D. Dose dependent response of injections of naked dsRNA in *M. sanguinipes*. E. Effect of oral feeding of naked dsRNA in *M. sanguinipes*. Bars represent different treatment groups. Three to five biological replicates and two technical replicates were used for RT-qPCR. For normalization, *EF1 α* and *Ubc10* were used as reference genes for *S. gregaria* and *RpL5* and *RpL32* for *M. sanguinipes*. The mRNA level in the treated group was relative to the control (*GFP*) group. Error bars indicate the standard error of mean. The statistical significance of differences was analyzed with Student's *t*-test or one-way ANOVA. Statistically significant differences between the control and target genes are indicated by different lowercase letters or asterisks (*: $P < 0.05$; **: $P < 0.01$). If no letters or asterisks are shown, no statistically significant differences were observed among treatments.

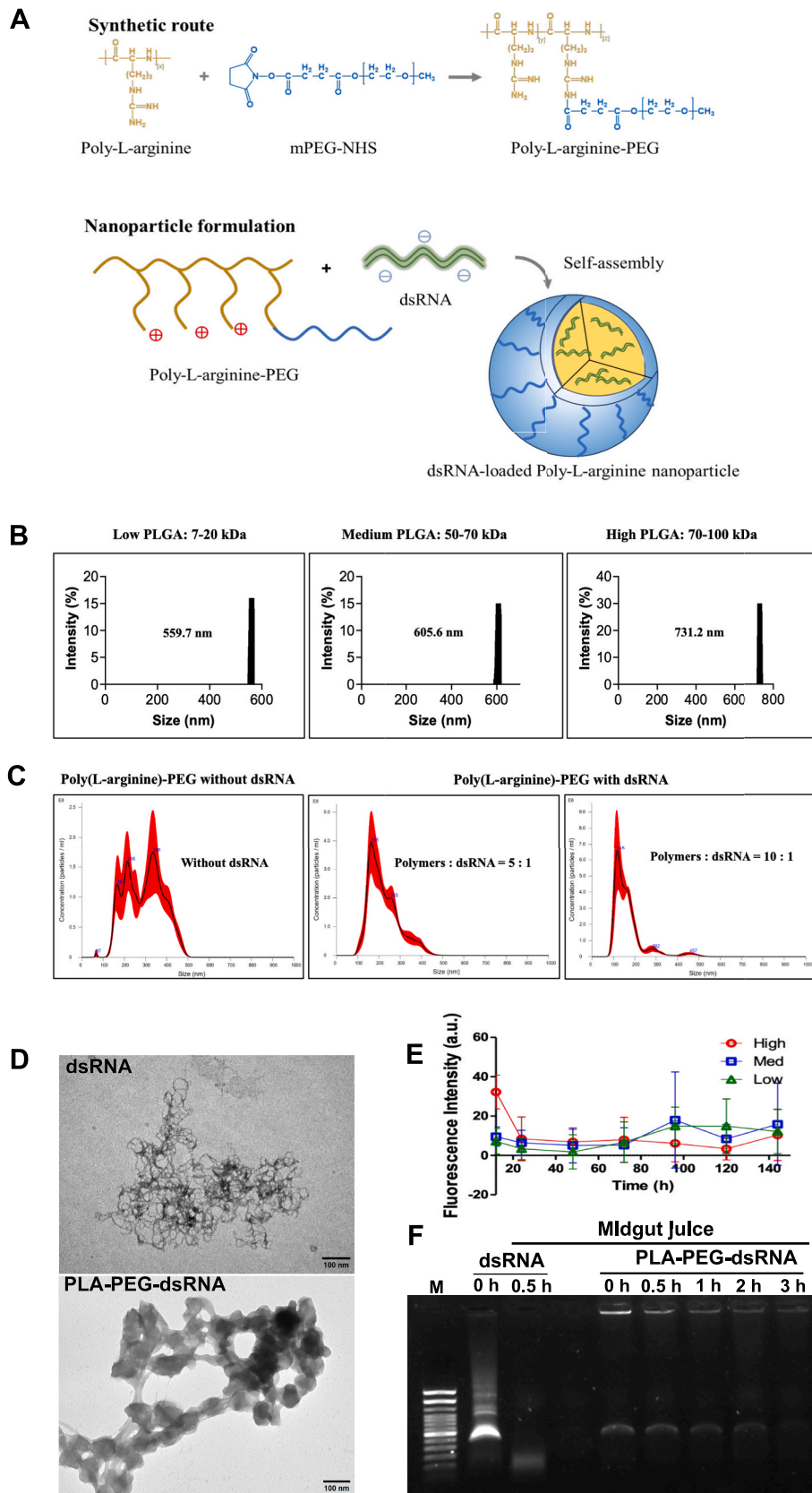


Fig. 2. Characterization of PLGA-dsRNA and PLA-PEG-dsRNA. **A.** Schematic representation of the generation process for PLA-PEG-dsRNA nanoparticles. **B.** PLGA particle size distribution. **C.** PLA-PEG particle size distribution and dsRNA complexation at various weight ratios of PLA-PEG:dsRNA (5:1, 10:1). **D.** Microscopic morphologies of naked dsRNA and PLA-PEG-dsRNA obtained by TEM. Scale bars = 100 nm. **E.** Release kinetics of coumarin from PLGA-coumarin in the hemolymph of *S. gregaria*. Low, Medium, and High refer to the molecular weights of PLGA. **F.** Agarose gel image of PLA-PEG-dsRNA stability assay in *S. gregaria* midgut juice.

significant knockdown effects were observed at all tested doses in *M. sanguinipes*, including the lowest dose of 50 ng (Fig. 1D), demonstrating the sensitivity of both species to injections and the presence of systemic RNAi effect. On the contrary, oral feeding of naked dsRNA did not produce any significant knockdown effects in either species for any of the tested genes or tissues (Fig. 1B, 1C, and 1E). Interestingly, in *S. gregaria*, a significant increase in expression of *GAPDH* was observed in the head tissue of the dsRNase2_GAPDH group (Fig. 1B). We also examined the mRNA level of *dsRNase2* in the midgut tissue of *S. gregaria*. The injected nymphs showed a significant knockdown of *dsRNase2* in the midgut for the dsRNase2_GAPDH group (Fig. 1A, 1C), while the fed nymphs did not show significant knockdown (Fig. 1B). Notably, the injected GFP_GAPDH group showed higher levels of *dsRNase2* (Fig. 1A, 1C).

3.3. Characterization of PLGA-dsRNA and PLA-PEG-dsRNA

The size and distribution of the PLGA-dsRNA nanoparticles using dynamic light scattering with a ZetaPALS particle size analyzer revealed a monodisperse size distribution, indicating successful encapsulation (Fig. 2B). For the PLA-PEG nanoparticle complexes, we determined the optimal complexation between dsRNA and PLA-PEG by varying weight ratios, and the nanoparticle tracking system analysis showed efficient complexation and uniform size distribution at a PLA-PEG:dsRNA weight ratio of 10:1 (Fig. 2C). The morphological structure of naked dsRNA appeared as long, thin threads, whereas the PLA-PEG-dsRNA formed well-defined spherical nanoparticles under TEM (Fig. 2D). The formation of these spherical nanoparticles suggests strong electrostatic interactions between the PLA-PEG and dsRNA, leading to condensation and structural collapse of dsRNA into compact nanoparticle assemblies.

3.4. PLGA-coumarin permeates the gut and is released in the hemolymph

We further characterized the release kinetics of coumarin dye encapsulated in PLGA nanoparticles of varying molecular weights. Coumarin was detected in the hemolymph of *S. gregaria* nymphs fed with PLGA-coumarin of all molecular weights (Fig. 2E), indicating that the PLGA successfully permeated through the gut and released the dye into the hemolymph. The highest coumarin fluorescence was observed at 12 h after the nymphs were fed with the high molecular weight PLGA, followed by the medium and low molecular weight PLGA (Fig. 2E). This pattern indicated that the larger particle size of high molecular weight PLGA (Fig. 2B) provided more surface area for initial coumarin release, leading to higher early release (from 12 to 72 h). After this period, the high molecular weight PLGA showed a slower and more sustained release, as its polymer started to hydrolyze more slowly compared to the faster hydrolysis of medium and low molecular weight PLGA, which showed higher coumarin release after 72 h, lasting until 144 h (Fig. 2E). Based on these results, higher molecular weight PLGA was selected for further oral feeding experiments due to its higher and sustained release. The same release pattern was observed in *M. sanguinipes*, where the high molecular weight PLGA also showed a higher initial release followed by a slower sustained release (Supplementary Fig. 1).

3.5. PLA-PEG enhances dsRNA stability in *S. gregaria* midgut juice

As shown in Fig. 2F, naked dsRNA was completely degraded within 30 min of incubation in midgut juice *ex vivo*. In contrast, dsRNA with the PLA-PEG complex remained detectable for up to 2 h, showing a gradual decrease in band intensity over time (Fig. 2F). This suggests that while some degradation occurred, the PLA-PEG complex provided significant protection and prolonged dsRNA stability in the midgut environment *ex vivo*.

3.6. No knockdown was observed with oral feeding of PLGA-dsRNA and PLA-PEG-dsRNA

To investigate whether PLGA-dsRNA and PLA-PEG-dsRNA could facilitate an RNAi response through oral feeding, we fed both types of nanoparticles to both insect species. However, no significant knockdown was observed in either insect species (Fig. 3A, 3B, 3C, 3D). In *S. gregaria*, we also tested whether the injection of *dsdsRNase2* could knockdown the mRNA expression of *dsRNase2* in the midgut by first assessing the persistence of knockdown across various time points. Interestingly, a significant knockdown of *dsRNase2* was observed at 48 h (25-fold change), 72 h (5.26-fold change), and 96 h (50-fold change) (Supplementary Fig. 2). Some level of knockdown was also observed at 24 h (1.64-fold change) (Supplementary Fig. 2).

Next, we tested if the initial *dsRNase2* knockdown through injection could reduce the dsRNA degrading activity in the midgut and whether subsequent feeding of PLGA-dsRNA could elicit RNAi response targeting *GAPDH*. As expected, injection of *dsdsRNase2* led to a significant knockdown of *dsRNase2* in the midgut (Fig. 3A). However, subsequent oral feeding of PLGA-dsGAPDH did not lead to the knockdown of *GAPDH* in the head and thorax tissues (Fig. 3A). Additionally, significantly increased expression of *dsRNase2* was observed in the GFP_GAPDH group (Fig. 3A), similar to what was observed with the injections of naked dsRNA in *S. gregaria*.

To explore further, we conducted additional experiments using PLA-PEG-dsRNA in *S. gregaria*, testing different doses and durations. We fed PLA-PEG-dsGAPDH at both high doses for short periods (Fig. 3C) and low doses for extended durations (Supplementary Fig. 3) to see if this could elicit an RNAi response through oral feeding. However, no knockdown of *GAPDH* was observed in any tested tissues at two time points (Fig. 3C, Supplementary Fig. 3).

Similarly, in *M. sanguinipes*, no knockdown was observed for any of the targeted genes upon oral delivery (Fig. 3D). Even after feeding 5 µg of PLA-PEG-dsRNA for five consecutive days, no significant knockdown was detected at either time point for any of the target genes, except for a slight but non-significant reduction in *Sec23* expression (Supplementary Fig. 4).

3.7. PLA-PEG-dsRNA permeates the gut and facilitates complex entry into fat body cells

Cy3 fluorescence was clearly observed in the fat body cells of both *S. gregaria* and *M. sanguinipes* (Fig. 4). The fluorescence signal was particularly stronger in *S. gregaria* compared to *M. sanguinipes* (Fig. 4).

4. Discussion

RNAi-based insecticides offer a multitude of advantages over conventional chemical counterparts. Moreover, RNAi's transient gene expression knockdown during key developmental stages minimizes long-term ecological consequences, a critical distinction from more radical approaches like gene drive systems. However, this approach faces challenges when scaled up for widespread pest management, especially for the generalist herbivores with chewing mouthparts, such as grasshoppers and locusts. The most feasible option for field-based insect pest control for these types of pests is through formulations that facilitate oral ingestion of dsRNA. Many studies have successfully applied dsRNA to plant leaves, allowing insects to ingest the dsRNA while feeding on treated foliage, or incorporated dsRNA into baits and artificial diets (Gordon and Waterhouse, 2007; Price and Gatehouse, 2008; Liu et al., 2020). Nonetheless, challenges remain, particularly concerning variable RNAi efficiency among insects upon oral dsRNA delivery (Cooper et al., 2019; Zhu and Palli, 2020). In this study, we show that the two orthopteran pests are highly sensitive to RNAi when dsRNA is delivered by injection (Fig. 1A, D), but are refractory to the oral feeding of dsRNA (Fig. 1B, E), even after the attempts to reduce the

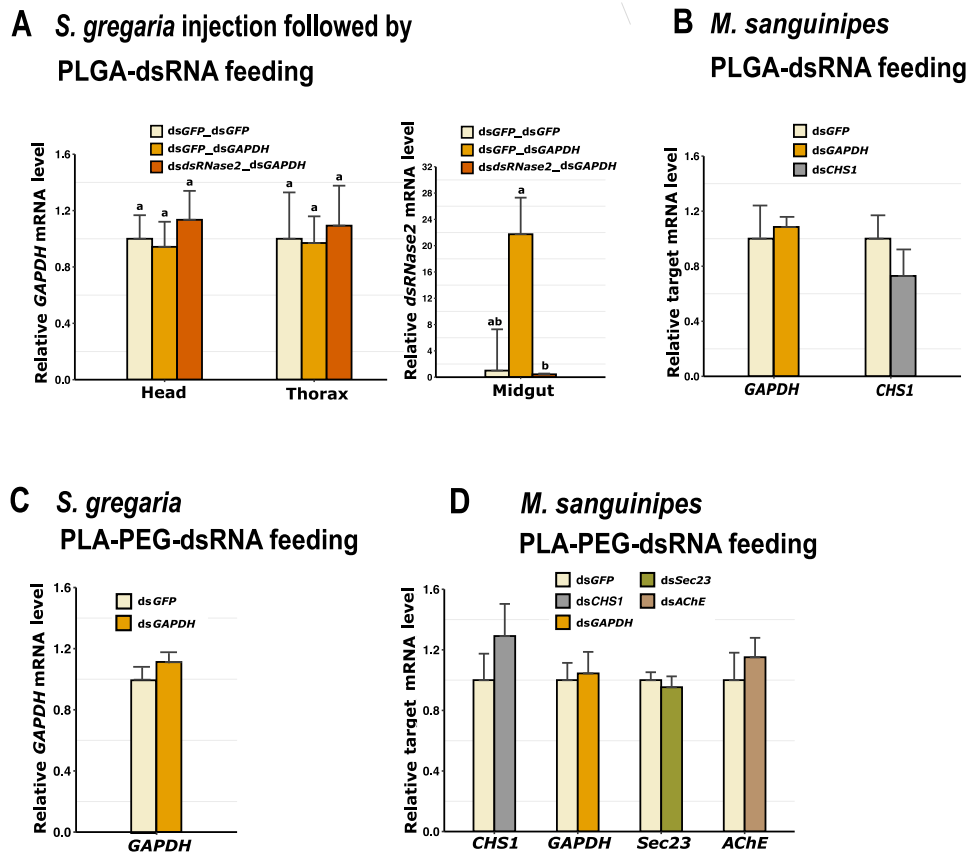


Fig. 3. Effect of oral feeding of PLGA-dsRNA and PLA-PEG-dsRNA in *S. gregaria* and *M. sanguinipes*. A. Effect of injection of *dsdsRNase2* followed by oral feeding of PLGA-dsGAPDH in *S. gregaria*. B. Effect of oral feeding of PLGA-dsRNA in *M. sanguinipes*. C. Effect of oral feeding of PLA-PEG-dsRNA in *S. gregaria*. D. Effect of oral feeding of PLA-PEG-dsRNA in *M. sanguinipes*. Bars represent different treatment groups. Three to five biological replicates and two technical replicates were used for RT-qPCR. For normalization, *EF1 α* and *Ubc10* were used as reference genes for *S. gregaria* and *RpL5* and *RpL32* for *M. sanguinipes*. The mRNA level in the treated group was relative to the control (*GFP*) group. Error bars indicate the standard error of mean. The statistical significance of differences was analyzed with Student's *t*-test or one-way ANOVA. Statistically significant differences between the control and target genes are indicated by different lowercase letters. If no letters or asterisks are shown, no statistically significant differences were observed among treatments.

presence of dsRNA-degrading enzymes in the midgut using the RNAi-of-RNAi approach (Fig. 1C). We also explored the potential for encapsulating dsRNAs using nanoparticles originally developed for drug delivery (Fig. 2A-D) and show that they permeate through the insect digestive system to reach the hemolymph (Fig. 2E), remain stable in the midgut juice (Fig. 2F), and are uptaken by the fat body (Fig. 4). However, despite these promising results, dsRNA-encapsulating nanoparticles did not lead to knockdown of target genes upon oral delivery (Fig. 3), suggesting that more work is needed to understand the molecular physiology of these insects.

Many insects show variable RNAi responses, and we clearly demonstrate that *S. gregaria* and *M. sanguinipes* are highly sensitive to the injection of dsRNA (Fig. 1A, D), suggesting the presence of systemic RNAi, but refractory to the oral administration of dsRNA (Fig. 1B, E). The reasons for this refractory nature could be many, but one of the most suggested for various insects is the presence of dsRNA-degrading enzymes (dsRNases) in the midgut (Song et al., 2017; 2019; Spit et al., 2017). For example, four types of *dsRNase* have been identified in *S. gregaria*, all of which are highly expressed in the midgut and share significant sequence similarity (Wynant et al., 2014). Wynant et al. (2014) showed that knocking down *dsRNase2* alone can reduce the expression of three other dsRNases. Based on this insight, we specifically targeted *dsRNase2* for our experiments. While we were able to successfully knockdown the expression of *dsRNase2* through the injection of *dsdsRNase2* (Fig. 1C), the subsequent oral delivery of dsRNA did not lead to knockdown (Fig. 1C).

Interestingly, with injections, the knockdown effect of *GAPDH* was

consistent regardless of whether *dsdsRNase2* was injected (Fig. 1A, D), suggesting that *dsRNase2* activity in the hemolymph did not significantly affect RNAi efficiency. However, when *dsRNase2* was knocked down by injection and followed by oral feeding of dsGAPDH, we observed no knockdown of *GAPDH*, further supporting the refractory nature of these insects to oral RNAi. We recovered a similar response in *M. sanguinipes*, showing high sensitivity to injected dsRNA but refractory to oral feeding of dsRNA. These responses also align with our previous work with another orthopteran often classified as a pest in the U.S., Mormon cricket (*Anabrus simplex* (Haldeman)) (Hoang et al., 2022; Rana et al., 2023). While we measured the relative dsRNase mRNA expression level, it is possible that residual dsRNase activity was sufficient to degrade the dsRNA after feeding. Additionally, the dsRNase domain structure varies across insect species (Cooper et al., 2019), potentially affecting enzyme activity and RNAi efficiency. Furthermore, while an endocytosis-mediated uptake mechanism has been reported in *S. gregaria* (Wynant et al., 2014), this mechanism has only been observed with injections. In the case of feeding, the dsRNA-uptake mechanism (binding proteins or receptors) may not necessarily be the same or even present in the gut. The presence of a peritrophic matrix, which is continuously secreted on feeding, may also prevent dsRNA from passing through the gut. We also observed an increase in the expression of *GAPDH* or *dsRNase2* in the head and midgut tissues, respectively (Fig. 1A-C, 3A). The increase in *GAPDH* expression appears to be tissue-specific (Fig. 1B), which could potentially be stress-induced. The increase in *dsRNase2* expression (Fig. 1A, 1C, 3A) is likely a viral defense mechanism, however, the increase was only observed in the

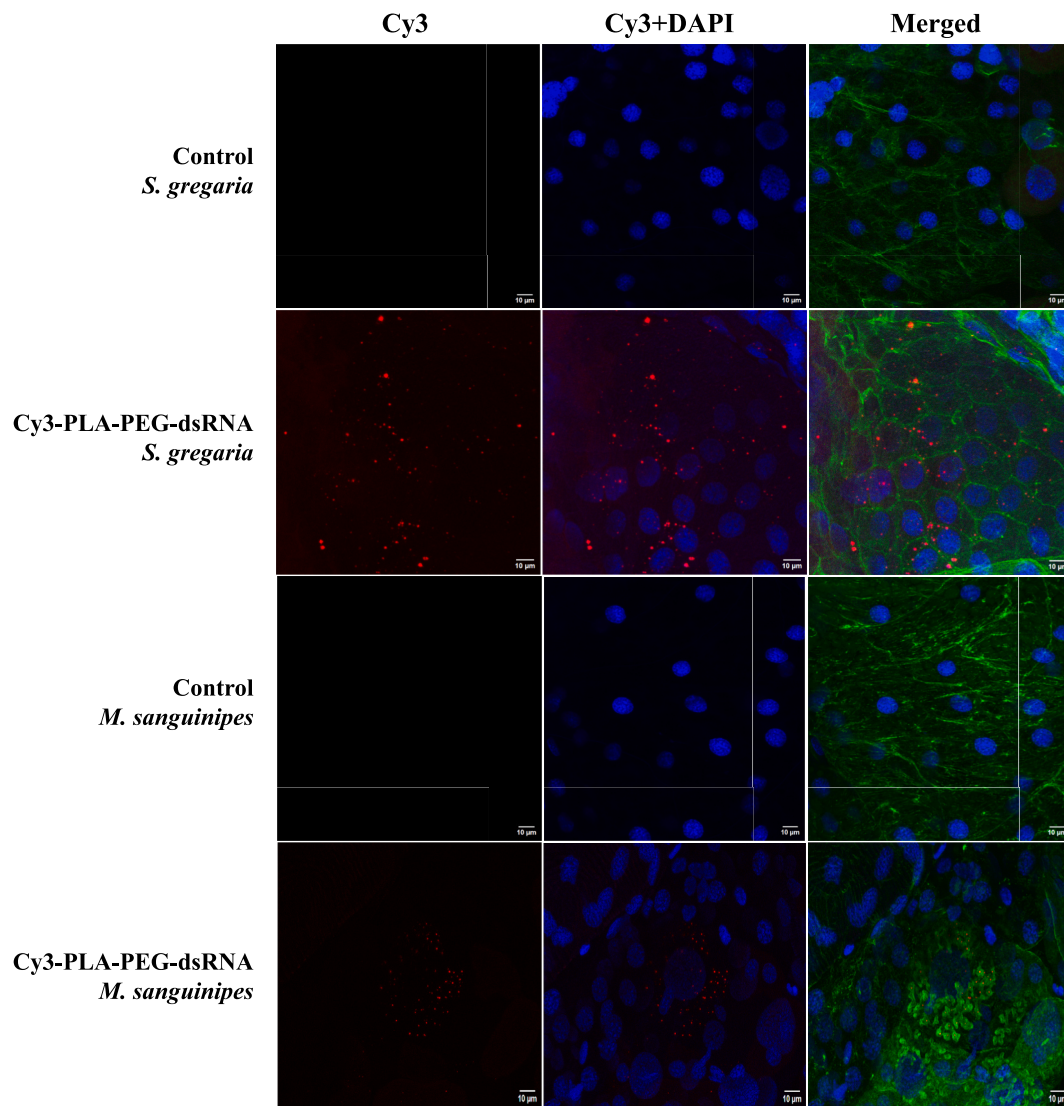


Fig. 4. Uptake of Cy3 labeled PLA-PEG-dsRNA into fat body cells of *S. gregaria* and *M. sanguinipes* at 24 h. Nymphs were orally fed with Cy3 labeled PLA-PEG-dsRNA, while non-fed nymphs were used as controls. Red fluorescence represents Cy3 labeled PLA-PEG-dsRNA, blue indicates nuclear staining (DAPI), and green shows actin staining (phalloidin). Scale bars = 10 μ m.

GFP_GAPDH group, suggesting a defense mechanism triggered specifically against dsRNA targeting endogenous insect genes rather than exogenous GFP. Additionally, there could be several possible factors for this variability, as reported in several insect species (Cooper et al., 2019), including *S. gregaria*, such as (1) High dsRNase activity in the gut due to favorable pH conditions; (2) Presence of other unknown nuclease-degrading enzymes in gut or saliva that are specific for orthopteran pests; (3) Inefficient or absence of dsRNA permeability and uptake mechanisms from the gut lumen; (4) Impaired endosomal escape if the dsRNA uptake mechanism through endocytosis exists; and (5) Unfavorable gut environment including pH, ions, metabolites, macromolecules, and/or digestive enzymes affecting the dsRNA stability in these orthopteran pests.

Our results collectively suggest that the dsRNase activity in the gut may not be a sole determinant of inefficient oral RNAi. This aligns with the findings in *S. gregaria* (Spit et al., 2017) and contrasts with the study in *L. migratoria*, where dsRNase2 knockdown improved RNAi efficiency following oral feeding (Song et al., 2017). While dsRNase activity is generally correlated with low RNAi efficiency, this relationship may not be universal, as some insect pests like Colorado potato beetle (*Lepidotarsa decemlineata*) exhibit high RNAi efficiency despite high

dsRNase activity (Spit et al., 2017; Singh et al., 2017).

Nanoparticle-based drug delivery has been widely used in the medical and pharmaceutical sciences, and their recent use in the development of COVID-19 vaccines to protect the mRNA from degradation with their efficient targeted delivery has increased their popularity. Over the past decade, these delivery methods provided attractive opportunities for testing in insect species, particularly to address the limitations of oral feeding (Zhang et al., 2010; He et al., 2013; Zhang et al., 2015; Christiaens et al., 2018; Edwards et al., 2020; Laisney et al., 2020; Lu et al., 2022; Vogel et al., 2023). In our study, we explored the potential of PLGA and PLA-PEG for encapsulating or conjugating dsRNA in the prospect of protecting dsRNA from an unfavorable gut environment and, in turn, eliciting the oral RNAi in *S. gregaria* and *M. sanguinipes*. We showed that PLGA-coumarin was permeable from the digestive system (Fig. 2E), consistent with our previous findings in Mormon cricket, but it was not stable in the midgut juice (Rana et al., 2023). In contrast, PLA-PEG-dsRNA showed both permeability through the digestive system and stability in the midgut juice (Fig. 2F, 4). However, neither nanoparticle complex elicited gene knockdown (Fig. 3A-D). These results suggest that nanoparticle permeability is not likely the primary limitation, as coumarin fluorescence was detected in the hemolymph of *S. gregaria*,

demonstrating that the nanoparticle complex was taken up (Fig. 2E). Moreover, it is unclear whether the entire nanoparticle complex is taken up by the cells or if only the coumarin dye is absorbed and released into the hemolymph.

Similarly, with the PLA-PEG-dsRNA nanoparticles, fluorescence imaging provided direct evidence that PLA-PEG-dsRNA permeated and was uptaken via the digestive system, followed by its release into the hemolymph, and subsequent localization in fat body cells (Fig. 4). These results highlight the potential of PLA-PEG nanoparticles to enhance the dsRNA uptake from the gut, facilitating systemic delivery within both insects. However, despite its uptake into the fat body, no RNAi response was observed in either insect species following oral feeding (Fig. 3C and 3D). This raises the question: if the uptake occurs, why does it not lead to an efficient RNAi response? One explanation may be that the uptake alone might not be sufficient to cause efficient RNAi. The alternative interpretation might be that the nanoparticle complex was not intact upon cellular uptake. Since the Cy3 is attached to the PLA, it is unclear from our uptake results whether the entire Cy3-PLA-PEG-dsRNA complex is internalized or if fragments: Cy3-PLA, Cy3, or Cy3-PLA-PEG are absorbed. Further experiments are needed to clarify these mechanisms and determine whether the entire PLA-PEG-dsRNA complex or only part of it is being absorbed. Interestingly, our results contrast with the studies on *L. migratoria*, where PEG-polylysine (thiol) [PEG-Plys(SH)] was shown to improve the oral RNAi (Lu et al., 2022). This suggests that the responses to nanoparticle formulations may be species-specific and not necessarily produce the same results across all insect taxa, highlighting the variability and complexity of the oral RNAi in different species.

In conclusion, our results highlight the challenges of oral RNAi in *S. gregaria* and *M. sanguinipes*. While the nanoparticle-based dsRNA delivery offers a promising approach to overcome these challenges, the barriers to oral RNAi are more complex than initially anticipated. Beyond dsRNase degradation and poor uptake, additional factors likely contribute to the refractory oral RNAi in *S. gregaria* and *M. sanguinipes*. Therefore, further studies are needed to address these challenges and optimize nanoparticle formulation for effective oral RNAi in these pest species.

CRediT authorship contribution statement

Seema Rana: Writing – review & editing, Writing – original draft, Visualization, Validation, Software, Project administration, Methodology, Investigation, Formal analysis, Data curation, Conceptualization. **Changsun Kang:** Writing – review & editing, Visualization, Validation, Methodology, Investigation, Formal analysis, Data curation. **Seonghyun Ryu:** Writing – review & editing, Methodology. **Derek A. Woller:** Writing – review & editing, Resources, Funding acquisition. **Dongin Kim:** Writing – review & editing, Resources, Investigation, Funding acquisition, Conceptualization. **Hojun Song:** Writing – review & editing, Supervision, Resources, Project administration, Methodology, Investigation, Funding acquisition, Conceptualization.

Declaration of competing interest

The authors declare that they have no known competing financial interests or personal relationships that could have appeared to influence the work reported in this paper.

Acknowledgments

We thank Lonnie R. Black and Travis Hitchner of the USDA-APHIS-PPQ-Science & Technology (S&T)-Insect Management and Molecular Diagnostic Laboratory's (Phoenix Station, AZ, United States) Rangeland Grasshopper and Mormon Cricket Management Team and Dewey Murray of USDA-APHIS-PPQ-Field Operations for their assistance in collecting the wild *M. sanguinipes* used for this research. We also thank Arianne Cease and Rick Overson of the Global Locust Initiative at

Arizona State University, AZ, United States for providing *M. sanguinipes* egg pods (funded by USDA-APHIS-PPQ-S&T Cooperative Agreement, FAIN AP19PPQS&TT00C217) to start our colonies. The authors acknowledge the assistance of the Integrated Microscopy and Imaging Laboratory and Malea Murphy at the Texas A&M College of Medicine, TX, United States. RRID:SCR_021637 and Image Analysis Laboratory and Joseph Szule at Texas A&M University, Veterinary Medicine & Biomedical Sciences, TX, United States RRID: SCR_022479. This research was supported by two USDA-APHIS-PPQ-S&T Cooperative Agreements (FAIN AP22PPQS&T00C021 and FAIN AP22PPQS&T00C023) funded by FY22 Plant Protection Act 7721 (to H. S., D.K. and D.A.W.), the U.S. National Science Foundation, United States (grant number DBI-2021795 to H.S.) and the USDA Hatch Grant, United States (TEX0-2-6584 to H.S.). This research may not necessarily express APHIS' views.

Appendix A. Supplementary data

Supplementary data to this article can be found online at <https://doi.org/10.1016/j.jinsphys.2025.104825>.

Data availability

Data will be made available on request.

References

- Alessandro, S.D., Fall, A.A., Grey, G., et al., 2015. Senegal agricultural sector risk assessment. World bank group report number 96296-SN. <https://documents1.worldbank.org/curated/en/238261468184467370/pdf/96296-WP-P1148139-Box393200B-PUBLIC-54055TAP-Senegal-ASRA-08262015-web-jtc.pdf>.
- Chomczynski, P., Mackey, K., 1995. Short technical reports. Modification of the TRI reagent procedure for isolation of RNA from polysaccharide- and proteoglycan-rich sources. *Biotechniques* 19 (6), 942–945.
- Christiaens, O., Tardajos, M.G., Reyna, Z.L.M., et al., 2018. Increased RNAi efficacy in *Spodoptera exigua* via the formulation of dsRNA with guanlylated polymers. *Front. Physiol.* 9, 316. <https://doi.org/10.3389/fphys.2018.00316>.
- Cooper, A.M.M.W., Silver, K., Zhang, J., et al., 2019. Molecular mechanisms influencing efficiency of RNA interference in insects. *Pest Manag. Sci.* 75 (1), 18–28. <https://doi.org/10.1002/ps.5126>.
- Edwards, C.H., Christie, C.R., Masotti, A., et al., 2020. Dendrimer-coated carbon nanotubes deliver dsRNA and increase the efficacy of gene knockdown in the red flour beetle *Tribolium castaneum*. *Sci. Rep.* 10 (1), 12422. <https://doi.org/10.1038/s41598-020-69068-x>.
- FAO. 2020. <https://www.fao.org/newsroom/story/Five-things-you-should-know-about-an-age-old-pest-the-Desert-Locust/en>.
- FAO. 2025. <https://openknowledge.fao.org/server/api/core/bitstreams/bb20c047-a494-45d1-82ce-88a2553cde60/content>.
- Gilding, D.K., Reed, A.M., 1979. Biodegradable polymers for use in surgery polyglycolic/poly(lactic acid) homo-and copolymers: 1. *Polymer* 20 (12), 1459–1464.
- Gordon, K.H.J., Waterhouse, P.M., 2007. RNAi for insect-proof plants. *Nat. Biotechnol.* 25 (11), 1231–1232. <https://doi.org/10.1038/nbt1107-1231>.
- Hausbergert, A.G., Deluca, P.P., 1995. Pergamon 0731-7085(95)01276-1 characterization of biodegradable poly(D,L-lactide-co-glycolide) polymers and microspheres. *J. Pharm. Biomed. Anal.* 13 (6), 747–760.
- He, B., Chu, Y., Yin, M., et al., 2013. Fluorescent nanoparticle delivered dsRNA toward genetic control of insect pests. *Adv. Mater.* 25 (33), 4580–4584. <https://doi.org/10.1002/adma.201301201>.
- Hoang, T., Foquet, B., Rana, S., et al., 2022. Development of RNAi methods for the Mormon Cricket, *Anabrus simplex* (Orthoptera: Tettigoniidae). *Insects* 2022, Vol. 13, Page 739. 13(8):739. <https://doi.org/10.3390/INSECTS13080739>.
- Joga, M.R., Zotti, M.J., Smaghe, G., et al., 2016. RNAi efficiency, systemic properties, and novel delivery methods for pest insect control: What we know so far. *Front. Physiol.* 7, 553. <https://doi.org/10.3389/fphys.2016.00553>.
- Laisney, J., Gurusamy, D., Elhaj Baddar, Z., et al., 2020. RNAi in *Spodoptera frugiperda* Sf9 Cells via nanomaterial mediated delivery of dsRNA: a comparison of poly-L-arginine polyplexes and poly-L-arginine-functionalized Au nanoparticles HHS Public access. *ACS Appl. Mater. Interfaces* 12 (23), 25645–25657. <https://doi.org/10.1021/acsami.0c06234>.
- Le Gall, M., Overson, R., Cease, A., 2019. A global review on locusts (Orthoptera: Acrididae) and their interactions with livestock grazing practices. *Front. Ecol. Evol.* 7, 263. <https://doi.org/10.3389/fevo.2019.00263>.
- Liu, S., Jaouannet, M., Dempsey, D.A., et al., 2020. RNA-based technologies for insect control in plant production. *Biotechnol. Adv.* 39. <https://doi.org/10.1016/j.biotechadv.2019.107463>.
- Livak, K.J., Schmittgen, T.D., 2001. Analysis of relative gene expression data using real-time quantitative PCR and the 2^{-ΔΔCT} method. *Methods* 25 (4), 402–408. <https://doi.org/10.1006/METH.2001.1262>.

- Lu, Q., Cui, H., Li, W., et al., 2022. Synthetic nanoscale RNAi constructs as pesticides for the control of *Locust Migratoria*. *J. Agric. Food Chem.* 70 (35), 10762–10770. <https://doi.org/10.1021/acs.jafc.2c04195>.
- Luo, Y., Wang, X., Wang, X., et al., 2013. Differential responses of migratory locusts to systemic RNA interference via double-stranded RNA injection and feeding. *Insect Mol. Biol.* 22 (5), 574–583. <https://doi.org/10.1111/imb.12046>.
- Makadia, H.K., Siegel, S.J., 2011. Poly lactic-co-glycolic acid (PLGA) as biodegradable controlled drug delivery carrier. *Polymers (Basel)*. 3 (3), 1377. <https://doi.org/10.3390/POLYM3031377>.
- Mitchell, D.J., Steinman, L., Kim, D.T., et al., 2000. Polyarginine enters cells more efficiently than other polycationic homopolymers. *J. Pept. Res.* 56 (5), 318–325. <https://doi.org/10.1034/J.1399-3011.2000.00723.X>.
- Murray, D.W., 2016. The Biology, Ecology, and Management of the Migratory Grasshopper, *Melanoplus sanguinipes* (Fab. :13. Available from <http://digitalcommons.unl.edu/entodistmastershttp://digitalcommons.unl.edu/entodistmasters/13>.
- Newsom, A., Koli, M., Sebesvari, Z., 2021. Technical Report: Locust Outbreak 2019–2021. <https://collections.unu.edu/view/UNU:9195>.
- Noh, S.M., Park, M.O., Shim, G., et al., 2010. Pegylated poly-l-arginine derivatives of chitosan for effective delivery of siRNA. *J. Control. Release* 145 (2), 159–164. <https://doi.org/10.1016/j.jconrel.2010.04.005>.
- Pfadt, R.E., 2002. Field Guide to Common Western Grasshoppers. 3rd edn. Wyoming Agricultural Experiment Station Bulletin. https://www.ars.usda.gov/ARSUserFiles/30320505/GH_pdfs/FieldGde.pdf [June 30, 2020].
- Price, D.R.G., Gatehouse, J.A., 2008. RNAi-mediated crop protection against insects. *Trends Biotechnol.* 26 (7), 393–400. <https://doi.org/10.1016/j.tibtech.2008.04.004>.
- Pugsley, C.E., Isaac, R.E., Warren, N.J., et al., 2021. Recent advances in engineered nanoparticles for RNAi-mediated crop protection against insect pests. *Front. Agron.* 9. <https://doi.org/10.3389/FAGRO.2021.652981>.
- Rana, S., Kang, C., Allred, J., et al., 2023. Differential responses to double-stranded RNA injection and feeding in Mormon cricket (Orthoptera: Tettigoniidae). *J. Insect Sci.* 23 (4), 10–11. <https://doi.org/10.1093/JISESA/IEAD063>.
- Robison, A.D., Sun, S., Poyton, M.F., et al., 2016. Polyarginine interacts more strongly and cooperatively than polylysine with phospholipid bilayers. *J. Phys. Chem. B* 120 (35), 9287–9296. https://doi.org/10.1021/ACS.JPCB.6B05604/SUPPL_FILE/JP6B05604_SI_001.PDF.
- Singh, I.K., Singh, S., Mogilicherla, K., et al., 2017. Comparative analysis of double-stranded RNA degradation and processing in insects. *Sci. Rep.* 7 (1). <https://doi.org/10.1038/s41598-017-17134-2>.
- Song, H., Fan, Y., Jianqin, Z., et al., 2019. Contributions of dsRNases to differential RNAi efficiencies between the injection and oral delivery of dsRNA in *Locusta migratoria*. *Pest Manag. Sci.* 75 (6), 1707–1717. <https://doi.org/10.1002/ps.5291>.
- Song, H., Jianqin, Z., Li, D., et al., 2017. A double-stranded RNA degrading enzyme reduces the efficiency of oral RNA interference in migratory locust. *Insect Biochem. Mol. Biol.* 86, 68–80. <https://doi.org/10.1016/j.ibmb.2017.05.008>.
- Sparks, T.C., Storer, N., Porter, A., et al., 2021. Insecticide resistance management and industry: the origins and evolution of the Insecticide Resistance Action Committee (IRAC) and the mode of action classification scheme. *Pest Manag. Sci.* 77 (6), 2609–2619. <https://doi.org/10.1002/PS.6254>.
- Spit, J., Philips, A., Wynant, N., et al., 2017. Knockdown of nuclease activity in the gut enhances RNAi efficiency in the Colorado potato beetle, *Leptinotarsa decemlineata*, but not in the desert locust *Schistocerca gregaria*. *Insect Biochem. Mol. Biol.* 81, 103–116. <https://doi.org/10.1016/j.ibmb.2017.01.004>.
- USDA APHIS 2019. Rangeland grasshopper and Mormon cricket suppression program, final environmental impact statement November 2019; 2019. https://www.aphis.usda.gov/plant_health/ea/downloads/2019/rangeland-grasshopper-mormon-cricket-program-final-eis.pdf.
- USDA APHIS 2024. <https://www.aphis.usda.gov/plant-pests-diseases/ghmc/grasshoppers-mormon-cricket-western-faqs>.
- Vogel, E., Santos, D., Huygens, C., et al., 2023. The study of cell-penetrating peptides to deliver dsRNA and siRNA by feeding in the desert locust, *Schistocerca gregaria*. *Insects* 2023, Vol. 14, Page 597. 14(7):597. <https://doi.org/10.3390/INSECTS14070597>.
- Wise, D.L., McCormick, G.J., Willet, G.P., et al., 1976. Sustained release of an antimalarial drug using a copolymer of glycolic/lactic acid. *Life Sci.* 19 (6), 867–873. [https://doi.org/10.1016/0024-3205\(76\)90314-3](https://doi.org/10.1016/0024-3205(76)90314-3).
- Wu, W., Liu, W., Wang, S., et al., 2008. Drug controlled release of novel alginate/poly-L-arginine microcapsules. *IFMBE Proc.* 19, 26–28. https://doi.org/10.1007/978-3-540-79039-6_7.
- Wynant, N., Verlinden, H., Breugelmanns, B., et al., 2012. Tissue-dependence and sensitivity of the systemic RNA interference response in the desert locust *Schistocerca gregaria*. *Insect Biochem Mol Biol.* 42 (12), 911–917. <https://doi.org/10.1016/j.ibmb.2012.09.004>.
- Wynant, N., Santos, D., Verdonck, R., et al., 2014. Identification, functional characterization and phylogenetic analysis of double stranded RNA degrading enzymes present in the gut of the desert locust *Schistocerca gregaria*. *Insect Biochem Mol Biol.* 46 (1), 1–8. <https://doi.org/10.1016/j.ibmb.2013.12.008>.
- Zhang, C., Tang, N., Liu, X.J., et al., 2006. siRNA-containing liposomes modified with polyarginine effectively silence the targeted gene. *J. Control. Release* 112 (2), 229–239. <https://doi.org/10.1016/j.jconrel.2006.01.022>.
- Zhang, X., Mysore, K., Flannery, E., et al., 2015. Chitosan/interfering RNA nanoparticle mediated gene silencing in disease vector mosquito larvae. *J. Vis. Exp.* 2015 (97), 52523. <https://doi.org/10.3791/52523>.
- Zhang, X., Zhang, J., Zhu, K.Y., 2010. Chitosan/double-stranded RNA nanoparticle-mediated RNA interference to silence chitin synthase genes through larval feeding in the African malaria mosquito (*Anopheles gambiae*). *Insect Mol. Biol.* 19 (5), 683–693. <https://doi.org/10.1111/j.1365-2583.2010.01029.x>.
- Zhu, K.Y., Palli, S.R., 2020. Mechanisms, applications, and challenges of insect RNA interference. *Annu. Rev. Entomol.* 65 (1), 293–311. <https://doi.org/10.1146/annurev-ento-0111019-025224>.